

Ion and Plasma Thruster Test Console Based on Three-Phase Resonant Conversion Power Modules

Geoffrey N. Drummond¹
Colorado Power Electronics, Inc., Fort Collins, CO 80524

John D. Williams²
Colorado State University, Fort Collins, CO 80523

Abstract

A test console is described for operation of both high power Hall-effect thrusters (HETs) and ion thrusters. The console utilizes three-phase resonant DC conversion power modules. It is believed that three phase resonant conversion (3PRC) of electrical power is ideally suited for EP power systems, and will soon become the premier converter for flight applications. These converters produce the lowest voltage ripple over any known topology. Additionally, they process power continuously and not in pulses as do their single phase predecessors. The absence of power pulses greatly reduces the size and mass of filter components in the three phase converter, and the smooth power transfer has helped it obtain peak efficiency ratings of >97%. Three phase resonant power converters are also wide ranging compared to competing designs. For example first-order CPE designs have exhibited efficiencies of 97% or higher at full power over an output impedance range of 4:1. Recently developed second-order CPE designs have achieved an output impedance range of 25:1 at efficiencies above 96%. A comparison of 3PRC to square-wave and single-phase resonant conversion is presented. A preliminary comparison is also provided of flash x-ray survivability of standard "current-fed" and 3PRC designs where x-ray pulse duration effects are considered. Another advantage of 3PRC modules over other power conversion hardware is their low specific mass. Attendant to high efficiency and low specific mass is the added benefit of relatively easy thermal management with minimal requirements on heat conduction pathways and thermal interfaces. In addition to presenting a review of the 3PRC design and recent prototype performance, a detailed discussion is provided of the test console design and hardware intended for operation of all SEP-based ion and plasma thrusters that are currently available at NASA centers and commercial aerospace companies. The secondary goal of the test console effort is the development of a modular control system that can be interfaced to any number of 3PRC power modules in a plug and play fashion. The full versatility of the 3PRC design can be applied in this approach to (1) maximize circuit design re-use (enabled by the 3PRC wide range capability), (2) minimize system mass (due to low 3PRC specific mass and light thermal interface requirements), and (3) maintain world-class performance. The 3PRC test console development described herein is intended to serve as a guide to the development of standardized architecture sub-systems intended for off-the-shelf flight hardware solutions to future EP applications.

¹ President and Director, 120 Commerce, Unit 3

² Assistant Professor, Mechanical Engineering, 1320 Campus Delivery, AIAA Senior Member

1.0 Introduction

The Deep Space 1 spacecraft launched on Oct. 24, 1998 utilized electric propulsion for its primary propulsion system. The propulsion system was developed under the NASA Solar Electric Propulsion Technology Application Readiness (NSTAR) project. This system included a 30-cm diameter ion thruster, a propellant feed and storage subsystem, a power processor unit (PPU), and a digital control interface unit (DCIU) [Bond and Christensen, 1999]. The NSTAR propulsion system was successfully operated for over 16 khr [Polk et al., 2001], and the success of this mission enabled JPL researchers to convince DAWN mission planners to utilize a three-thruster version of the NSTAR propulsion system for their spacecraft [Brophy et al., 2004]. The Discovery-class DAWN spacecraft will use the ion propulsion system to rendezvous with two near Earth asteroids- Vesta and Ceres.

Discovery class programs impose higher quality control requirements in comparison to a technology demonstration program like Deep Space I. These constraints have played a part in increasing the cost of the PPU and DCIU as design changes and component upgrades were implemented and difficulties related to these changes were encountered. Some of the root causes of these problems can be better understood by examining Bond and Christensen's [1999] photographs of the NSTAR PPU with its cover plate removed. Although there are two locations where additional power supply capacity could be installed, there is very little room to implement these options. A more ergonomic design would be to lay out the power supply system in a slice (or modular) packaging scheme. This choice would allow easy access to individual slices for initial assembly and re-work. In addition, the sub-assembly slices could be acceptance tested prior to insertion into the PPU. The output power could also be scaled using a modular/slice-based layout if the chassis is designed for expansion. Finally delta-qualification tests could be performed at the module-level to further reduce the costs of customization required by future interplanetary or asteroid rendezvous missions. The test console approach described herein utilizes a modular layout to take advantage of this design choice.

Another basic implementation-related challenge of the NSTAR PPU and DCIU is the physical separation of the two devices. The single-fault tolerant DAWN ion propulsion system requires two DCIUs and two PPUs. Integration of the DCIU into the PPU into a single device would result in a simpler system that would be easier to mate to the future spacecraft. Although desirable, an entire PPU re-design with embedded DCIU functionality is not easy to accomplish under current and foreseeable future financial constraints. And this is especially true when higher performance systems are needed. The goals of the work described herein is to (1) develop a low-cost, ground-based test console system using industry standard approaches that implements SOA power conversion designs, (2) validate the test console through extensive operation of NASA and commercial thrusters, and (3) systematically transition the test console sub-systems into flight qualified designs. Secondary goals of the test console development effort are to standardize and reduce the cost of flight acceptance and qualification performance tests by developing automated test sequences.

It is believed that three phase resonant conversion (3PRC) of electrical power is ideally suited for EP power systems, and will soon become the premier converter for flight applications. The benefits of 3PRC are just now receiving attention. These converters produce the least possible voltage ripple over any known topology. Additionally, they process power continuously not in pulses as do their single phase predecessors. The absence of power pulses greatly reduces the size and mass of filter components in the three phase converter. The 3PRC converter exhibits smooth current flow on input and output lines without filtering. The smooth power transfer of this new class of converter has helped it garner the high efficiency ratings of >97% [Kay, 2005] with low output stored energy.

Figure 1 shows the primary current for each of the three phases. When these three currents are summed together they produce a low ripple input current that is shown at the top of Fig. 1. It should be noted that the ripple frequency is six times higher than the switching frequency, and filtering of the remaining ripple is trivial. Three phase converters operating at an input of 100V only require 1- μ F of bus filter capacitance per kilowatt of output power. The bus capacitor for a 2.5-kW three phase converter should weigh less than two grams.

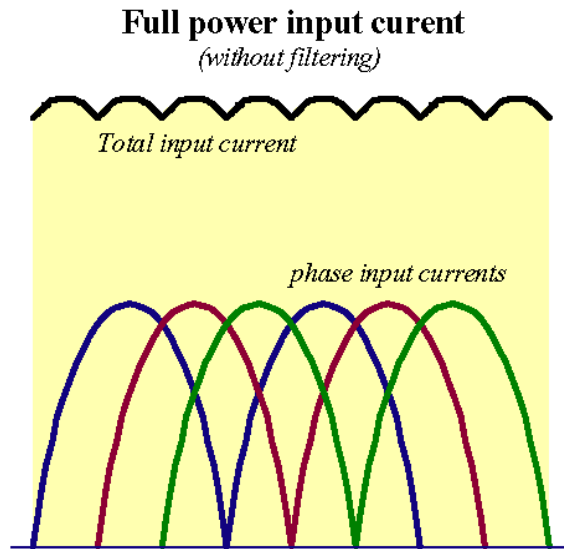


Fig. 1 Phase current and composite input current.

Additional benefits of 3PRC converters include:

- Wide load range output allows operation over two to one voltage range at full power and high efficiency, and simple circuit modifications extend the voltage range to 5:1.
- Inherent low stored energy allows safe operation of standard and advanced carbon-based ion optics systems by limiting charge transfer levels to < 1-mC.
- Low stored energy buss stability simplifies power buss architecture.
- Higher reliability, soft-switching components have fewer failure modes compared to hard switching devices used in currently available PPU designs.

Three phase resonant conversion was originally pioneered by one of the authors (GD) in the early 1990's. Since that time 3PRC has become the premier power converter for the thin film sputtering industry [cg., Drummond, 1996; Drummond and Hesterman, 2004]. Presently 10-kW modules are the most common size and are sold in 20-kW units for less than fifty cents per watt. This converter is currently the market leader in high power DC sputtering processes.

Our paper is organized into three major sections. The first section presents a typical test console layout scheme for moderate power ion thruster applications. Detailed descriptions of sub-system components are also described in this section. The second section presents a review of three phase resonant conversion where the unique features of this topology are identified and its applicability to electric propulsion applications are presented. The final section of the paper compares 3PRC to various existing power conversion topologies. A preliminary analysis is also presented in this section that identifies important circuit features required for improving survivability to long duration x-ray flash events, which is important for space-based power conversion systems. Finally, conclusions and recommendations for future work are drawn.

2.0 Typical CPE Test Console Layout and Sub-system Description

The test console system approach described in this paper is intended for, but not limited to (1) high power and high specific impulse ion thrusters in the NEXIS, HiPEP, and Herakles-class; (2) moderate power and moderate specific impulse ion thrusters in the NSTAR, XIPS-25, enhanced-NSTAR, and NEXT class; and (3) HETS in the H6, HiVAC, BPT4000, BHT HD and RT class. In addition, related wide-ranging laboratory and prototype devices at power levels up

to and beyond 150 kW are appropriate for 3PRC-based test consoles. As a typical example, this paper will focus on the description of a moderate power level (10 kW) and lower voltage (200-2000 V) test console intended for ion thrusters, which is referred to as the CPE IPX. A brief list of power supply characteristics is summarized in Table 1, and the detailed current/voltage characteristics of each supply are listed in Figure 2.

TABLE 1. Current and voltage definitions of test console power supplies.

Supply	Differential Voltage Range	Maximum Current (source)	Maximum Continuous Power
Discharge Ignitor Supply	10 VDC to 750 VDC	3A @ 50V to 20mA@750V	150 W
Discharge Heater Supply	4 VDC to 40 VDC	10A @ 40V to 20A @ 20V	400W
Discharge Supply	5 VDC to 50 VDC	20A @ 50V to 40A @ 25V	1000W
Screen Supply	200 VDC to 2000 VDC	5A @ 2kV to 10A @ 1kV	10kW
Neutralizer Heater Supply	4 VDC to 40 VDC	10A @ 40V to 20A @ 20V	400W
Neutralizer Ignitor Supply	10 VDC to 750 VDC	3A @ 50V to 20mA@750V	150W
Accel Supply	110 VDC to 1100 VDC	1.8A @ 550V to 0.91A @ 1.1kV	1000W

A block diagram of the CPE IPX test console is shown in Fig. 3. The dedicated control DACs identified along the left side of the figure are intended for use in managing processes that are either too important or are occurring too fast to be relegated to slower software control. The arc control DACs include (1) a timer used to quickly shutdown the screen and accelerator power supplies when an arc is detected, (2) conductance detectors on the screen and accelerator power supplies to monitor load changes that might be related to an arc event, and (3) a simple current spike detector for redundant arc detection should the conductance detectors malfunction. The arc detection circuitry enables the test console to discriminate and report electrical breakdowns that occur between the screen supply and ground, between the accelerator supply and ground, and between the screen and accelerator electrodes.

The power control DACs include (1) current control of the discharge and neutralizer keeper supplies, (2) current and voltage control of the discharge and neutralizer heater supplies, (3) voltage control of the the screen and accelerator supplies with secondary control of the maximum allowable current, and (4) current control of the discharge supply under nominal operation and during recycle turn-back conditions. Any user commands and all fault conditions not related to the arc and power control DACs are relegated to software control. The typical minimum time to respond to a software control command is 0.5 seconds. The inclusion of a decelerator electrode current measurement circuit was added to accommodate thrusters equipped with 3-grid ion optics systems. All voltages are referenced to the neutralizer cathode potential; however, the neutralizer cathode voltage-to-test facility ground is also monitored, and, consequently, all voltages are convertible to values referenced to test facility ground.

A high-efficiency, 10-kW module is the baseline for the screen power supply in ion thruster applications and for the anode power supply in HET applications. Two recent 10-kW breadboard units were fabricated with peak output voltages of 800 V and 2000 V. These units are also capable of delivering full output power at 400 V and 1000 V, respectively, and lower voltage operation is possible at lower output power levels. This was done to size all components for the (1) higher output current that operation at lower voltages would impose on a 10-kW power supply and for the (2) higher voltage stresses that are present at 2 kV. Related CPE test consoles have been operated up to 18 kV routinely and up to 65 kV in some instances. Figure 4 contains an efficiency contour map that was measured with the 10-kW screen module operated at the optimum input voltage condition. A very high efficiency of 97% was recorded at full power over a wide output impedance range (from 16 to 64 Ω).

IPX power converter load lines

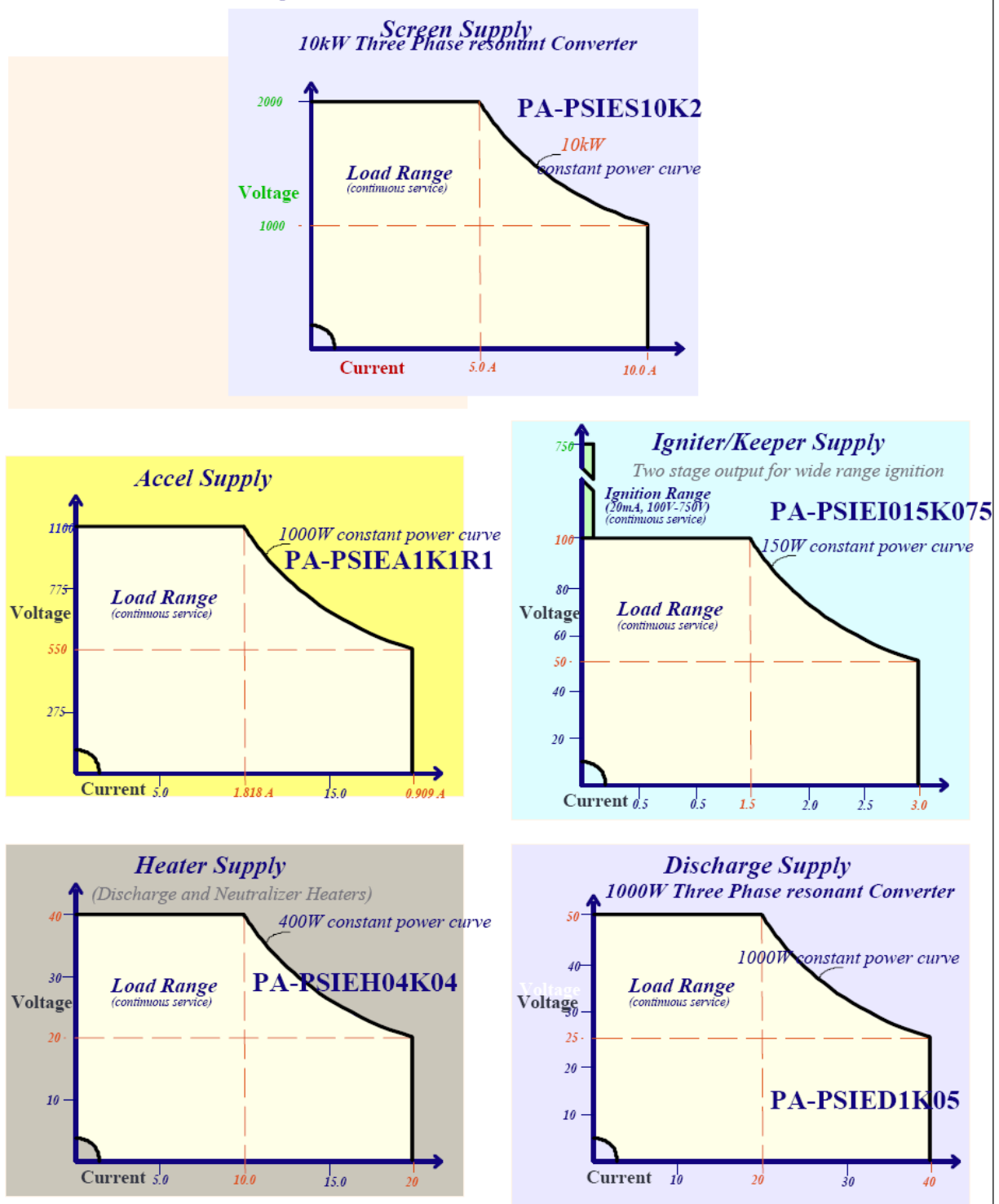


Fig. 2 Load lines for the seven power supplies of the CPE IPX test console.

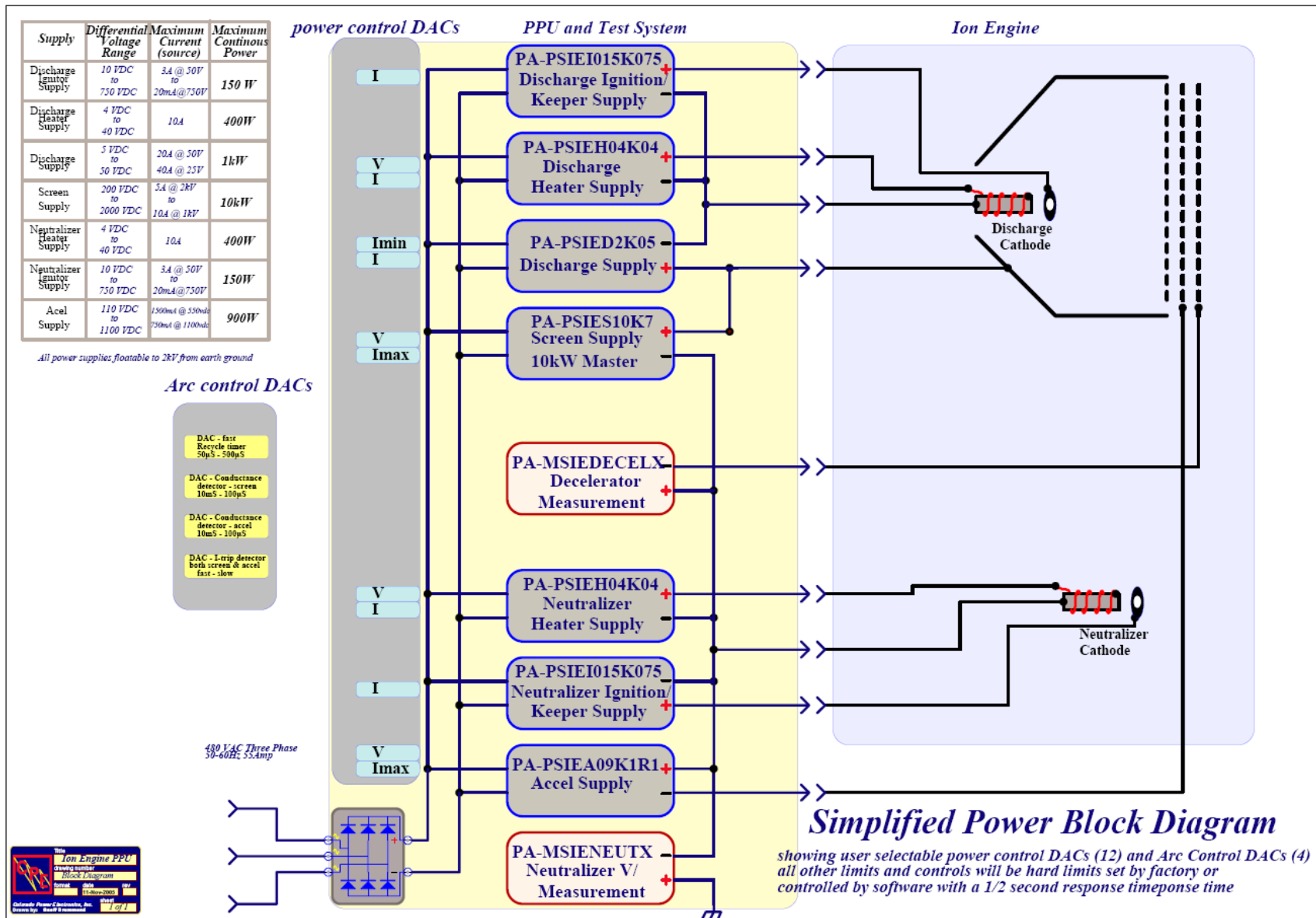


Fig. 3 Block diagram of entire system.

The 10-kW screen module breadboard (shown schematically in Figs. 5 and 6) is comprised of an input converter stage that utilizes MOSFET transistors and frequency selective elements, a three-phase transformer stage, and a diode rectifier output stage. The MOSFET transistors in the input converter produce square waves that have a fixed 120° phase shift. The square waves are converted to sine waves by frequency selective resonant circuit elements. Next, the three, phase-shifted sine waves are feed to a Delta-Wye transformer for voltage amplification where they produce a continuous flow of power to the load. The 120° phase shift is maintained as the frequency of the input conversion stage is varied to control power flow. As mentioned above, when the three-phase-shifted currents are summed together they result in a low ripple input current that minimizes the size of input filter capacitors. For the breadboard 10-kW module, the input filter capacitors only weighed ten grams. A 10-kW converter based on conventional topographies would require much heavier input filter capacitors. In addition, the lower buss energy of the input filter of the IPX screen module design improves the converter's survivability to flash events, which is important for space-based test console designs.

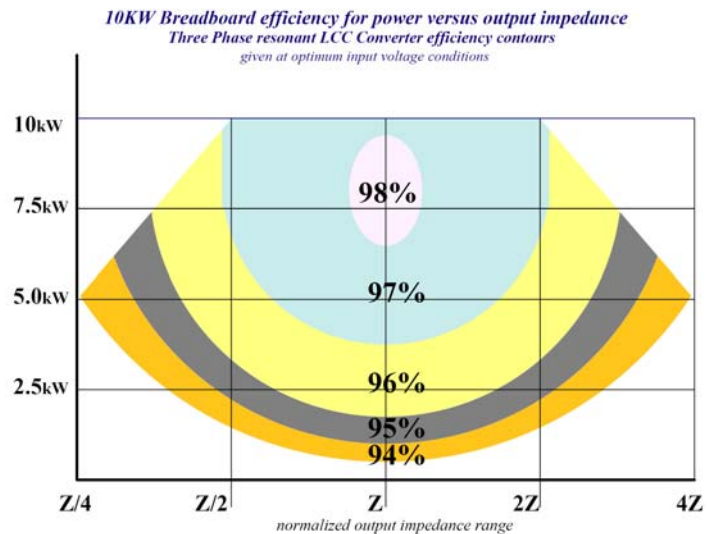


Fig. 4 Efficiency contour plot for the 800 V prototype 10-kW 3PRC power supply.

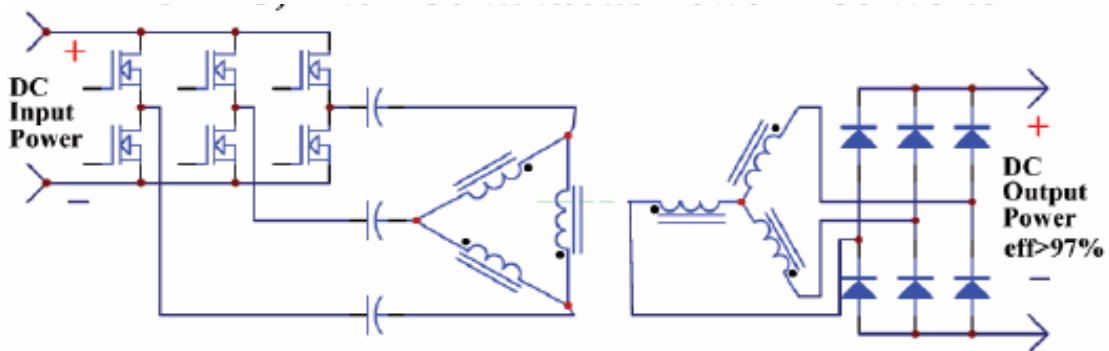


Fig. 5 Simplified circuit diagram of a three phase resonant converter.

**10kW Three Phase resonant Converter
with ripple reducing 12 pulse rectification**

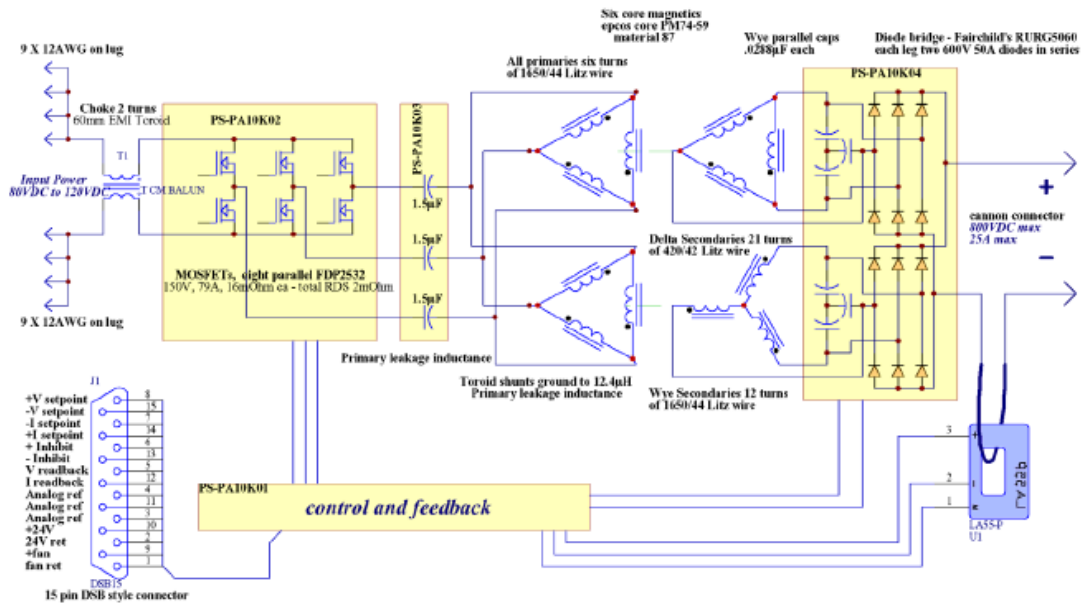


Fig. 6 Detailed circuit diagram of a three-phase resonant converter.

The low voltage 10-kW module shown in Fig. 7 performed satisfactorily over (1) an output voltage range of 400V to 800V DC at an output power level up to 10 kW and (2) over a DC input buss voltage of 80 to 120 V DC while maintaining an efficiency greater than 96%. Although high efficiency operation of the ground-based IPX test console is not necessary, it will allow use of simple air-cooling processes. The final mass of the low voltage 10-kW screen module was only 11 kg including all packaging and air-cooling equipment, which helps minimize the overall size and weight of the IPX test console. Note that the specific mass of 1.1 kg/kW is four times lower than high power space-based power processor units.

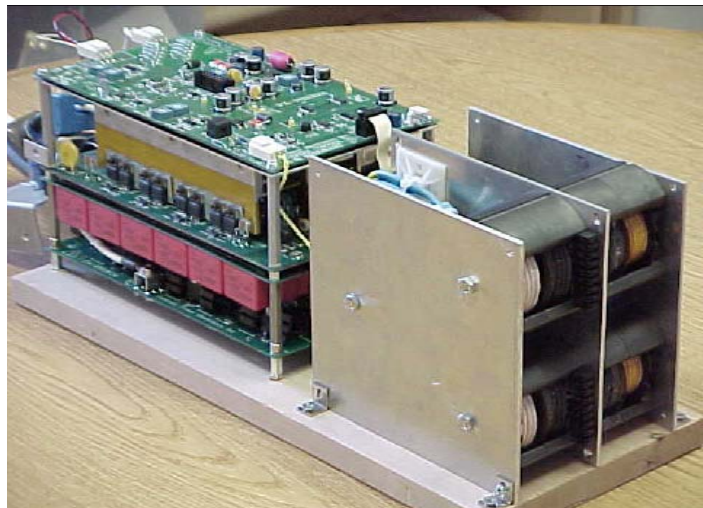


Fig. 7 Low voltage 10 kW module shown without cover. Mass 11 kg. Peak eff. 97.9% at full power.

A brief description of the sub-system components used in the 10-kW power module shown in Figs. 6 and 7 is given below. One specific design objective of the 10-kW module input stage was to develop circuitry for parallel MOSFETs operation (up to 8) that conserves energy and is resistant to parallel FET oscillations. A gate drive input stage circuit was developed that used active shunt transistors for the following benefits: (1) Lower drive power. The shunt transistor current subtracts from the required drive current yielding lower input current to the driver. (2) The active shunt resistors drive to 0.05 Ohms. This low impedance increases the

insertion losses to the MOSFETs thus reducing the tendency for parallel FET oscillation. And (3) ‘On to off’ gate transition is faster than with pure transformer derived gate pulses.

A printed circuit board (PCB) was designed for the input stage to ensure low inductance interconnection into the screen module to minimize losses associated with magnetic stored energy. The MOFET-based board is capable of handling 120 A, and a six-layer PCB layout was chosen that had a copper thickness of four ounces per square foot to accommodate these high currents. The foils of the PCB were interlaced to form a low inductance power buss to three half-bridges with eight parallel FETs per switch.

The 10-kW module was designed with a control board that includes a three-phase voltage controlled oscillator (VCO) circuit, output current and voltage control loops, a user interface, and output measurement circuitry. The series resonant capacitors (located between the input stage outputs and the transformer inputs) are also placed on a specially designed PCB with low inductance foil interconnects. These are the elements that are used in the frequency selective feature of the 3-phase resonant conversion scheme.

The rectifier diodes used in the output stage are configured in a three-phase, full-wave rectification layout that included parallel resonant capacitors. This topography results in a 12-point, balanceable output that has inherently low ripple content. The oscilloscope traces shown in Fig. 8 contain output voltage waveforms obtained with the output diode board in both balanced and un-balanced states.

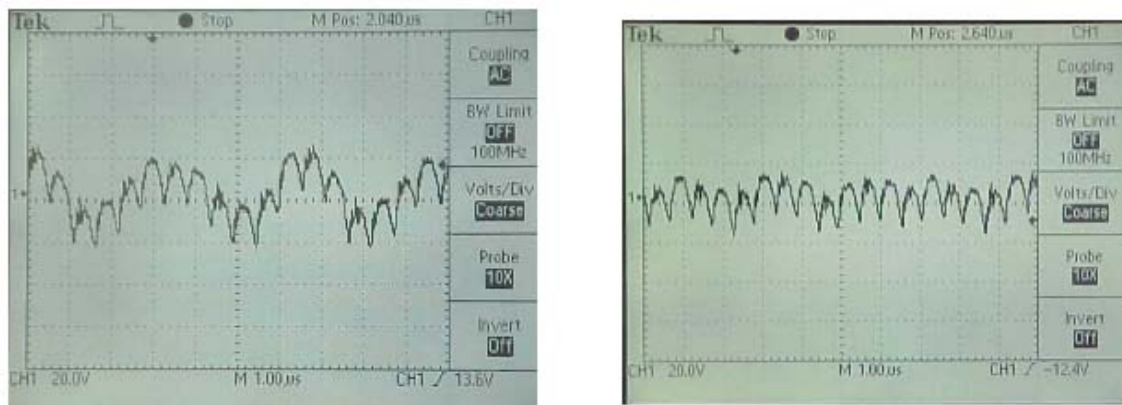


Fig. 8 Output ripple at 500 V before balancing (left) and after balancing (right). Note that the 5% ripple result was obtained with no output capacitance. The 2 MHz output AC content is a result of the twelve-point rectification scheme and is easy to eliminate with a small output cap.

Figure 9 contains a collection of CPE power conversion modules, control boards, and computer interface equipment that make up the IPX test console. Common computer communication busses are supported by the LCD-based controller including RS232, RS485, RS422 and GPIB. A state machine-based computer algorithm is used to perform all power supply operation and data acquisition tasks.

An ultra-wide range (voltage range of 5:1 and impedance range of 25:1) CPE converter was developed recently that can be dropped into the CPE IPX test console for added functionality, and Fig. 10 contains a series of photographs of a HET-like plasma source that was operated at power levels ranging from 30 W to 1000 W. The CPE converter was also found to safely operate the plasma load over a wide range of flow rate from 4 to 14 sccm (Xe), and no plasma source operational conditions were found that caused the CPE converter to improperly operate the plasma load. Figure 11 contains efficiency versus output voltage measurements before and after a round of circuit optimization steps were performed. An impressive level of efficiency (>96%) was achieved at full power over a voltage range of 5:1.

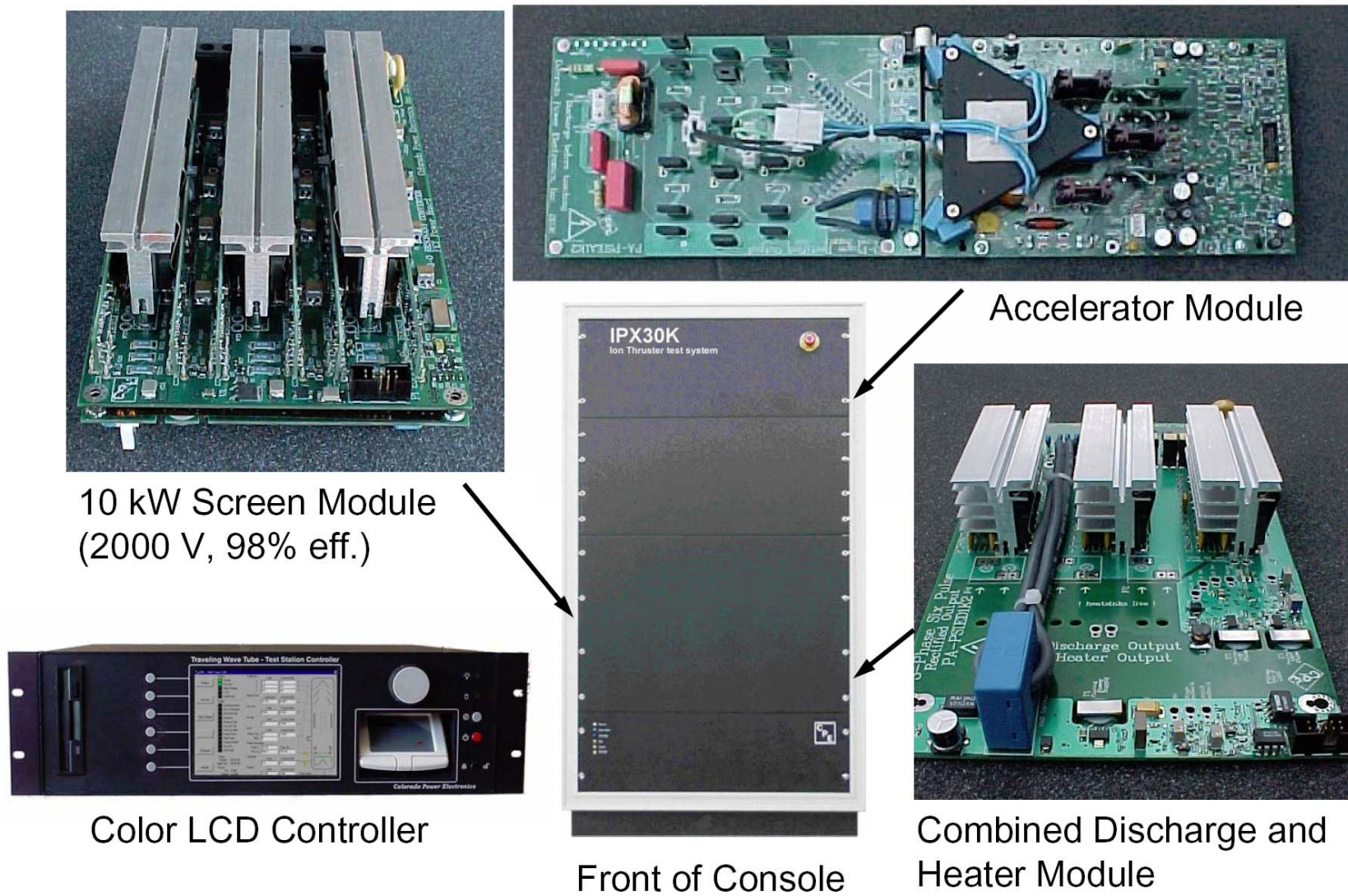


Fig. 9 Photographs of 3PRC modules used in the CPE IPX test console.

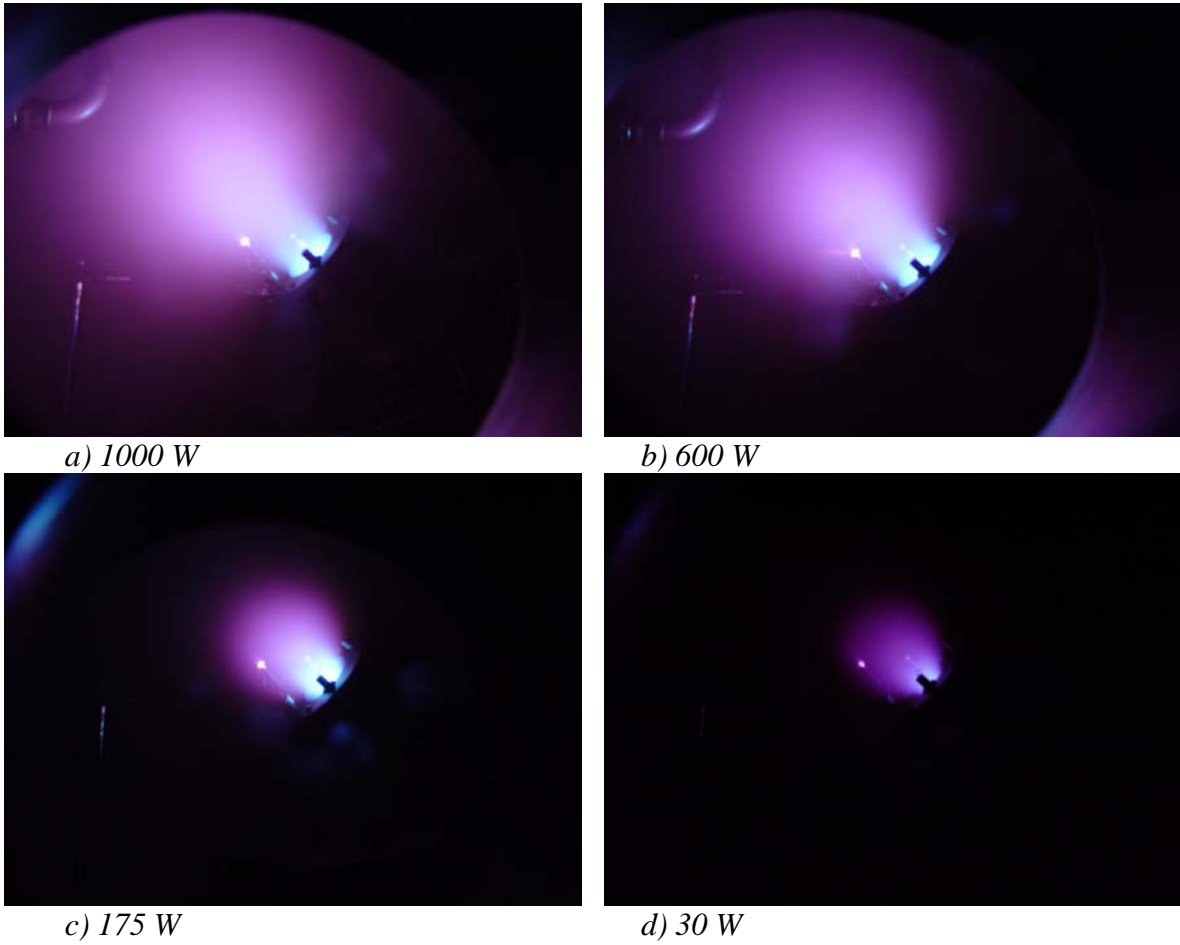


Fig.10 Photographs of HET-like plasma source operated with the CPE wide ranging power supply at power levels ranging from 30 to 1000 W.



Fig.11 Efficiency as a function of output voltage for the CPE 5:1 wide ranging power supply. The red data points were obtained after optimization of the 3-phase resonance circuits. All data shown were obtained at a constant output power level of 1 kW.

3.0 Three Phase Resonant Power Conversion

As mentioned above, a new converter topology has recently emerged that provides significant improvements in both efficiency and specific mass when compared to the present art of power conversion. The three-phase resonant converter (3PRC) described herein obtains its superior performance, in part, through a power conversion technique called soft switching. Many of today's power converters that claim soft switching do so only with the semiconductor switches and not with the output rectifiers. The LCC resonant components used in 3PRC guarantee soft-switching in both the power switches and rectifier diodes. Because of the soft-switching characteristics of all of the power devices, components can be added in parallel without concern about increased parasitic capacitance. Power MOSFETs and diodes can then be oversized to reduce current stress and increase overall efficiency. The ability to handle excess capacitance makes 3PRC the ideal converter for scaling power in electric propulsion applications.

3PRCs have been used in the thin film coating industry for more than ten years where they are currently the market leader. This converter topology is particularly known for low-stored energy, which is about 1-mJ per kilowatt of converter output power. It is noteworthy that the 3PRC design from CPE is a leading converter for ion engines equipped with low-arc-energy-tolerant carbon grids. Through this recent research it has become apparent that 3PRC efficiency is superior to that of the square-wave converters presently being developed for in-space propulsion applications. This discovery breaks a long held misconception that resonant converters are not as efficient as square-wave converters.

Figures 5 and 6 show the basic elements of the 3PRC, DC-DC converter. In Fig. 6, DC input voltage power enters on the left side of the diagram. The DC input voltage is then converted into three phase AC by the power switches. The frequency of the AC voltage is controlled to allow power flow through the resonant elements. The required resonant inductor is not drawn but is included as 'leakage inductance' in the magnetic assemblies. The secondary output voltages are developed across the parallel resonant capacitors and a full-wave rectifier circuit. The output of the rectifier circuit is a composite of the three phases and contains very little AC output ripple – even without filter capacitors. A twelve-pulse rectifier output is shown in Fig. 6, however, a simpler six-pulse rectifier can suffice in most applications. It is important to note the connection between the parallel resonant capacitors and the rectifier diodes. These capacitors are responsible for the soft-switching characteristics of the rectifier diodes. The capacitors also make the power circuit insensitive to the parasitic capacitance of the rectifier diodes.

The best recorded efficiency for 3PRC is more than one percentage point higher than the best reported efficiency for other high power converter topologies [Kay, 2005]. Or conversely the second place holder has 50% more waste power thus making them a distant second when important heat rejection considerations are made. In addition to beating the efficiency record by a wide margin, 3PRC has another extremely useful feature-- wide output voltage range at full power. As indicated in Figs. 4 and 11, the 3PRC can develop full- rated power transfer into impedance ranges of 4:1 to 25:1. This wide output range is achieved with high power factor (utilization) of the power components which means the losses remain nearly fixed as the full power output voltage is varied over the currently demonstrated 2:1 to 5:1 ranges.

4.0 Comparison of 3PRC Topology to Other Power Conversion Techniques

This section contains a comparison of several power conversion schemes along with a discussion of how power converters are affected by x-ray flash events that can be generated from either natural or man-made causes.

4.1 Square Wave Conversion, Multi-Phase

• Square wave power converters use semiconductor switches to produce square or rectangular waves from a DC input voltage. These waveforms are characterized by rapid rise and fall times and followed by periods of steady voltage called pulse top and pulse bottom. These square-waves are then processed by a transformer for load isolation and impedance matching. The transformer circuit then couples into a rectifier circuit where pulsing DC voltage is created. The AC component of this pulsing DC voltage is subsequently removed in the output filter to yield a DC output voltage. The square-wave converters used for PPU's are operated with switching frequencies in the 15 kHz to 50 KHz range. Higher switching frequencies are possible but usually come at the cost of reduced efficiency. The steep sides of the square-waves used in this type of power conversion are rich in harmonics frequencies that must be damped with lossy snubber circuits to prevent voltage overshoots that may damage semiconductors. Additional limitations come from diode recovery losses which must also be snubbed with a lossy clamp circuit.

All single-phase power converters process power in pulses. Single-phase power converters need physically large input and output filters to remove the voltage ripple caused by this pulsing power. To reduce the negative effects of the 'pulsed power' conversion some designs place several single-phase converters in parallel and stagger the power pulses to simulate constant power transfer. Most of the designs using parallel square-wave converters fail to capture the full advantages of multi-phase conversion due to inherent limitations of square-waves in power conversion. The first and most serious disadvantage of today's multi-phase conversion is that the parallel converters are not closely integrated. That is they are operating mostly as separate single-phase converters with only an output connector as a common element. The difference would be the same as comparing one six-cylinder gasoline engine to six one-cylinder engines with a common drive shaft. The second notable disadvantage of multi-phase square-wave is that output ripple changes shape and amplitude as the operating voltage is changed. Because the square-wave changes shape then so does the output ripple. For this reason power delivery with this circuit is not as continuous as it could be if sine-waves were used instead of square-waves.

4.2 Single-Phase, Series Resonant Power Conversion

Single phase resonant power conversion offers a significant improvement over single-phase square-wave conversion in these important areas:

1. Higher efficiency due to smooth power transfer and snubber-less designs.
2. Wider output range due to the highest efficiency point occurring in the middle of the load range.
3. Smaller size due to higher switching frequencies.
4. Higher demonstrated robustness with noisy plasma loads.

The list of advantages of the single-phase resonant converter makes it a clear winner over the square-wave converter. However, for high power designs, it is not the best possible converter as it still has the limitation of pulsing power. For high power applications continuous power delivery makes the most sense. When looking at power conversion techniques used for automobiles one quickly finds that multi-cylinder engines completely dominate the market. No one would give serious consideration to a design that used a one cylinder gasoline engine, or several single-cylinder engines with a common drive shaft. The nearly continuous power delivery of a multi-cylinder, single-block engine makes it the best choice for high power

automotive applications. The same principles apply for 3PRC as they do for the multi-cylinder gasoline engine. The 3PRC does not need to store and retrieve energy because it processes the power continuously. For low power applications where the best performance is not required the single-phase resonant converter is a good choice. The square-wave converter is only a good choice when the simplest converter is needed and efficiency is unimportant.

4.3 Preliminary Comparison of Flash Survivability of Common Circuit Topologies

PPUs for both military and commercial applications need to endure environmental radiation, but military applications require added protection against the prompt ionizing radiation that accompanies a nuclear explosion. Military applications for PPU's require demonstrated immunity from prompt and gamma ray radiation due to detonation of a nearby nuclear weapon. This prompt radiation is capable of causing large photo-currents in all semiconductor devices. The radiation itself produces little damage to the semiconductors; it is the system capacitors and batteries that contain the destructive energy. The radiation impulse triggers the release of the system's stored energy which in turn causes the irreversible damage to sensitive semiconductors. To prove resistance to damage from flash X-ray, special test equipment called simulators have been used to simulate the prompt dose of radiation found in a nuclear explosion.

It is considered practical by many equipment designers that one PPU design should be used for all applications; military and commercial. This is because the cost of qualifying electronic equipment for space applications is significant and warrants the reuse of hardware whenever possible. To this end it has been proposed that only a special class of power converters, namely "current-fed" power converters, should be considered for both military and commercial applications. Current-fed power converters such as the Clarke and Weinberg converter have been judged by some to have superior resistance to semiconductor photo-currents caused by prompt nuclear or x-ray radiation.

4.3a Myth of Flash Surge Protection with Current-Fed Designs in Real Situations

Current-fed power converters are really voltage-fed converters that contain current limiting elements. Because semiconductors can be destroyed more easily from excess voltage than from excess current, all converter designs need to limit the input voltage with some amount of input capacitance. The Weinberg Converter shown in the left side of Fig. 12 is a unique blend of two power converter techniques. It is the most popular of the current-fed designs for space flight applications and for this reason it is being analyzed in this discussion of current-fed designs. The transformer T1 is part of a "fly-back" converter and T2 is part of a "push-pull converter." The Weinberg converter places the inputs of the two converters in series while connecting their outputs in parallel. The combination of the fly-back and push-pull converters gives the Weinberg the constant input current property of a fly-back converter plus the power through-put capability of a push-pull converter. The current limiting property of T1 reduces rectifier stress and improves durability to transistor cross-conduction.

It is generally assumed that all semiconductors are susceptible to heavy photo diode conduction during flash radiation. And diodes and transistors with physically large die areas are prime candidates for short circuiting during radiation. The right side of Fig. 12 shows how a prompt burst of radiation affects the Weinberg Converter. For simplicity all the semiconductors are replaced with a wire indicating their conductive (or short circuit) state.

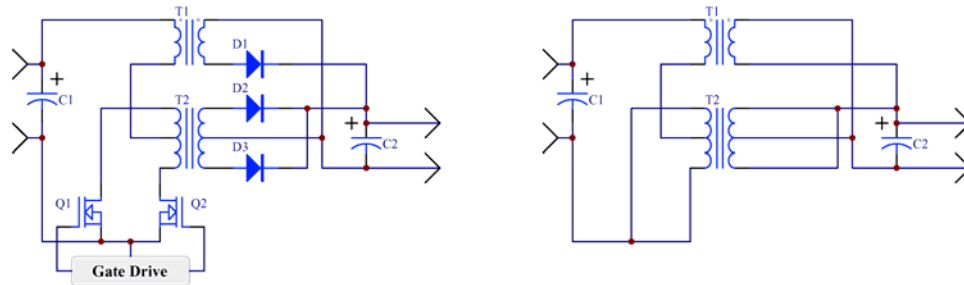


Fig. 12 Weinberg Converter, left. Simplified Weinberg converter during flash X-ray, right.

During a flash event the magnetizing inductances of the two transformers become short circuited by transistors Q1 and Q2 and diodes D1, D2, and D3. At this time only the leakage inductance of the Weinberg transformer is available to impede the building surge currents.

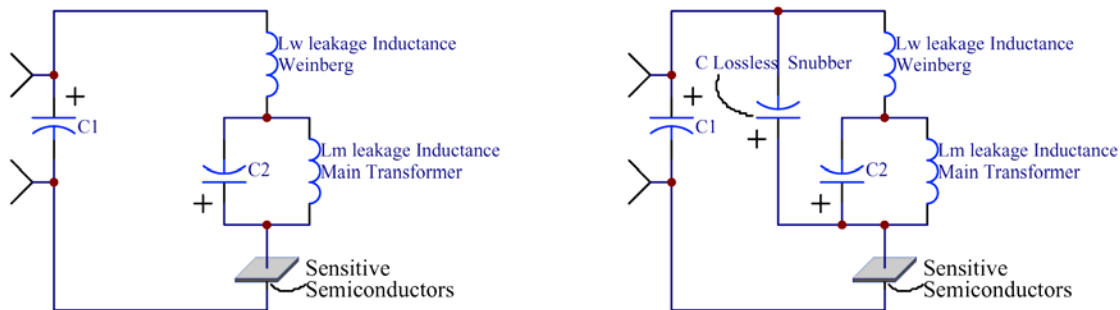


Fig. 13 Simplified Transformer Weinberg Converter, left. Simplified Weinberg converter with a common “lossless Snubber” added to the circuit model, right.

Figure 13 left, shows the simplified Weinberg converter with the short circuited magnetizing inductances omitted, leaving only the leakage inductance. Note that the output capacitor, C2, can inject its charge backwards through the circuit and into the shorted transistors.

A popular “lossless snubber” typically used with Weinberg Converters to limit voltage stress on the transistors turns into a deadly energy reservoir during flash X-ray events. This is because the snubber’s diodes become short circuited during the flash and the circuit shown in the right side of Fig. 13 is formed. Note that the snubber capacitor that once protected the transistors becomes a dangerous object during this upsetting event.

With only the scanty leakage inductance of the Weinberg transformer limiting the photo current, the current builds rapidly. Within one to two microseconds the transistor current builds to destructive levels. *After a few microseconds the current fed Weinberg converter has no advantage over any other converter design in regard to flash robustness.* Additionally, lossless snubbers may actually be weakening the Weinberg converter by allowing the snubber’s charge to add to the transistor’s photo current.

In manmade x-ray flash events, the duration of radiation in space is largely determined by the blackbody radiation lifetime of the fireball, generally regarded to last longer than 10 ms. This will vary greatly with the type and size of the device being detonated. *Simulators of flash radiation try to produce the dose rate of radiation that would be received in a typical detonation but not the duration of the radiation (i.e., effects of total dose are only studied by repetitively pulsing the simulator at relatively low duty).* The duration of radiation for most simulators of a flash X-ray event lasts less than 1 μ s. This is due to the nature of the simulator design and does not represent the expected duration of radiation during a manmade or natural event.

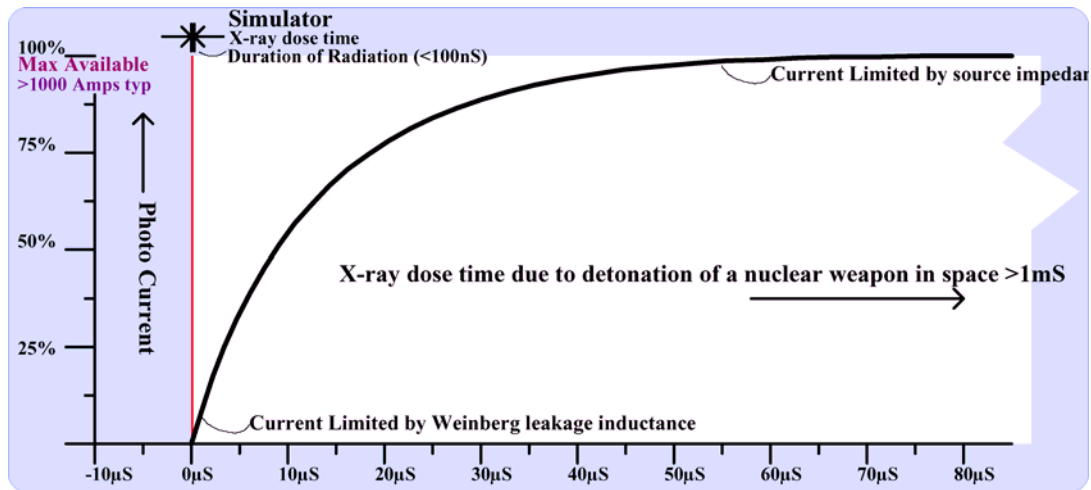


Fig. 14 Overall photo current in a Weinberg Converter during a flash event.

Figure 14 shows the expected Weinberg converter's input current during an actual blast from a nuclear weapon. The line in red shows the duration of a typical simulator radiation pulse. The area in pink, shown extending off of the page shows the expected duration from an actual flash x-ray event. Note that with the simulator the Weinberg converter experiences only a minor increase of photo current. But when comparing the currents of an actual event it becomes obvious that the converter offers no special protection against surging currents and subsequent destruction as the radiation duration exceeds 50 µs.

As a general note it appears that the level of robustness of the Weinberg is better than most other square-wave designs when driving a plasma load, and the Weinberg converter may offer robustness to square-wave conversion that is needed in the day-to-day operation of plasma based electric thrusters. However, it is far from being considered the best plasma power generator when compared to the emergent 3PRC technology. Furthermore, the 3PRC design may be the best candidate for x-ray flash solutions due to its inherent low stored energy. Since it is the stored energy devices that contain the destructive energy, it is our contention that low stored energy leads to durability in regard to flash events, however, more analysis and circuit simulation work needs to be performed to demonstrate this premise.

5.0 Conclusion and Recommendations for Future Work

The LCC series resonant-based 3PRC converter has a long list of demonstrated advantages and a short list of disadvantages. The period of discovery is still young for this new converter; and the list of improvements presented here is presumed by the authors to be partial and incomplete. The unique performance capabilities uncovered to date may represent only a small portion of the possibilities of the LCC topology, 3PRC design, and the 3PRC derivative products. Today's power system designers would think it to be impossible for a converter to handle a twenty-five to one load range. But it is now possible with highly efficient resonant conversion. When tomorrow's designers become aware of these emerging technologies, new applications and topology-variants will become available. For now both ion and Hall-effect thruster-based systems can benefit immediately from increased throttle range due to a new wide range PPU. The performance of the three phase resonant power converter, when compared to others, is impressive. Although impressive, the road to broad acceptance for in-space propulsion applications is still in front of this technology. One important obstacle in the path to universal acceptance is human prejudice, which is often confused with preserving heritage and sustained by failure to re-examine perceived strengths of existing devices. Ancient map makers were

known to scrawl “Thar be dragons beyond here” on the margins of their maps when areas unknown to them are included in the area being described. This was done to warn others of possible danger when entering these areas. One area in power conversion where there is currently a good deal of misunderstanding and possible danger is in prompt radiation simulation and how it represents (or more appropriately misrepresents) actual events that would be encountered in space. We should be wary here because current flash-event simulator technology has led to the poorly formed opinion that only bulky, low-efficiency, current-fed converters should be considered for space PPU designs. We have shown that actual flash x-ray events (of duration 10 μ s and longer) cause the current-fed converters to become ineffectual at protecting even the most robust electronic circuitry. And we point out here that there may be practical solutions to the problem of flash x-ray survivability when one utilizes circuit topologies with inherently low stored energy. A strong recommendation for future work would be to perform circuit analysis and simulations on a variety of power conversion technologies. Perhaps one solution for a system using a solar panel power source would be to configure the solar panels as energy crowbars. A large area solar panel array when combined with the low stored energy converter would form a damage resistant combination that may survive real x-ray flash events of long (>10 μ s) duration.

Acknowledgment

This work is supported in part by a NASA Phase II SBIR administered by the Jet Propulsion Laboratory. This support is gratefully acknowledged. Our appreciation is expressed to Mr. Marc Palmer, Mr. Eric Scheel, and Mr. Derek Krise for their careful craftsmanship in fabricating and testing the magnetic and electronic assemblies described herein. Also special thanks are extended to Ms. Teresa Krise for conducting the administrative details related to this work.

References:

- Bond and Christensen [1999]
T.A. Bond and J.A. Christensen, “NSTAR Ion Thrusters and Power Processors,” NASA/CR-1999-209162, Nov. 1999.
- Brophy et al [2004]
J.R. Brophy, G.B. Ganapathi, C.E. Garner, J. Gates, J. Lo, M.G. Marcucci, and B. Nakazono, “Status of the DAWN Ion Propulsion System,” AIAA-2004-3433, 40th Joint Propulsion Conference, Fort Lauderdale, FL, July, 2004.
- Drummond [1996]
G.N. Drummond, “Multi-phase DC Plasma Processing System,” US Patent #5,535,906, July 16, 1996.
- Drummond and Hesterman [2004]
G.N. Drummond and B.L. Hesterman, “Wide Range DC Power Supply Utilizing Voltage Doubling Output Capacitors and Inductive Choke to Extend Full Power Load Impedance Range,” US patent #6,697,265, Feb. 24, 2004.
- Kay [2005]
R. Kay, Private communication, Aerojet Corporation, Redmond Operations, Sept. 2005.
Independent evaluation of CPE hardware with Aerojet-owned, NIST-calibrated equipment. Peak efficiencies were found to be 98.3% at 2/3 power levels. Quoted 97% efficiencies are at full power for the 1-kW test article.
- Polk et al [2001]
J.E. Polk, et al., “Demonstration of the NSTAR Ion Propulsion System on the Deep Space One Mission,” IEPC-01-075, 27th International Electric Propulsion Conference, Pasadena, CA, Oct. 2001.